Astronomy & Astrophysics manuscript no.
(DOI: will be inserted by hand later)

The topology and polarisation of subbeams associated with the 'drifting' subpulse emission of pulsar B0943+10 — V. a new look at the low frequency 'B'urst-mode emission

Svetlana A. Suleymanova[1,3] and Joanna M. Rankin[2]

[1] Pushchino Radio Astronomy Observatory, 142290, Pushchino, Russian Federation, e-mail: suleym@psn.ru
[2] University of Vermont, Vermont, USA, e-mail: Joanna.Rankin@uvm.edu
[3] Isaac Newton Institute of Chile, Pushchino Branch

Abstract. This paper reports of new observations of pulsar B0943+10 carried out at the Pushchino Radio Astronomy Observatory (PRAO) at the low radio frequencies of 42, 62 and 112 MHz. B0943+10 is well known for its exquisitely regular 'B'urst-mode drifting subpulses as well as its weak and chaotic 'Q'uiescent mode. Earlier Arecibo investigations at 327 MHz have identified remarkable, continuous changes in its 'B'-mode subpulse drift rate and integrated-profile shape with durations of several hours. These PRAO observations reveal that the changes in profile shape during the B-mode lifetime are strongly frequency dependent—namely: the measured changes in the component-amplitude ratio are more dramatic at 327 and 112 MHz as compared with those at 62 and 42 MHz. The differences, however, are most marked during the first several 10s of minutes after B-mode onset; after an hour or so the profile forms at all four frequencies tend to be more similar. We also have found that the linear polarization of the integrated profile increases continuously throughout the lifetime of the B mode, going from hardly 10% just after onset to some 40-50% after several hours. While refraction in the pulsar's magnetosphere may well have a role, we find that the various effects, changing circulation time, frequency-dependent profile changes and increasing linear polarization, can best be understood as due to a moderate but systematically varying emission height within the polar flux tube.

Key words. MHD, plasmas, pulsars: radiation mechanism, polarization, mode-changing phenomenon

I. Introduction

Pulsar B0943+10 is well known for its 'B'urst mode, characterized by accurately drifting subpulses, in contrast with its chaotic 'Q'uiet mode. Every analysis of the star's B-mode properties has resulted in the conclusion that the observed subpulse drift is produced by a circulating pattern of precisely 20 'beamlets'. Thus, the B-mode subbeam-carousel circulation time can be computed as $\hat{P}_3 = 20\ P_3$, where P_3 is the inverse of the true drift-modulation frequency. Derived from intensity-fluctuation spectra, this modulation is known to present in general as a first-order alias of its true value. The pulsar's $\hat{P}_3$ time was determined initially using a B-mode sequence from the Arecibo Observatory (hereafter AO) and found to be about 37 stellar rotation periods (hereafter P_1) in average (Deshpande & Rankin 1999; 2001, hereafter Paper I). Asgekar & Deshpande 2001, hereafter Paper II) then confirmed it, remarkably, at the very low frequency of 35 MHz using observations from the Gauribidinur Observatory. Within the framework of the polar cap model (Ruderman & Sutherland, 1975), the subpulse 'drift' phenomenon is thought to result from a system of hot 'sparks' that precess around a star's magnetic axis feeding copious and relativistic primary plasma into discrete columns in the 'open' magnetosphere above them.

The methods of Papers I and II were then applied to a unique set of simultaneous dual frequency observations at 103 and 40 MHz acquired at the Pushchino Observatory (hereafter PRAO) and the results reported in Paper III of the series (Rankin, Suleymanova & Deshpande 2003). The intriguing correlation between the shapes of the B-mode average profiles and their corresponding circulation times $\hat{P}_3$ was identified. $\hat{P}_3$ values computed from fluctuation spectra of particular pulse sequences (hereafter PS) were found to exhibit correlated variations, further supporting the geometrical character of the drifting phenomenon in

Send offprint requests to: Dr. Suleymanova, e-mail: suleym@psn.ru

B0943+10. Subbeam carousel maps of B-mode PSs constructed using the 'cartographic' transformation at 430 and 111.5 MHz (Paper I), 35 MHz (Paper II) and at 103/40 MHz all resemble each other closely in consisting of a vigesimal beam system. However, the corresponding beamlet patterns of the 103- and 40-MHz simultaneous observations were surprisingly only weakly correlated.

The short duration of the PRAO PSs from the observatory's transit BSA and DKR-1000 instruments had left many questions unanswered about the overall modal dynamics in B0943+10. However, new AO 327-MHz observations (in 2003) with durations of 2+ hours have opened a new stage in the investigation of the star's modal process (Rankin & Suleymanova, hereafter Paper IV). These have revealed remarkably continuous changes in the integrated-profile shape and subpulse driftrate with a characteristic time of about 1 hour. B-mode circulation times are found to be some 36 P_1 just after onset and to exhibit an exponential relaxation to an asymptotic value of some 38 P_1 over the next several *hours*! It is now clear that the pulsar's usual B-mode profile—a conal double form with a bright leading and weak trailing component—represents an asymptotic state long after B-mode onset. The relative amplitude of the second component is observed to change dramatically at meter wavelengths from some 1.7 near onset to an asymptotic value of about 0.2. We find that the subbeam-carousel circulation time ($\hat{P}_3$) and the amplitude ratio $A(2/1)$ of the two components are closely related, such that one can be estimated reliably from the other. This striking regularity of B-mode behaviour, apparently recurring similarly after every modal onset, has no parallel know in other normal isolated pulsars.

Here, in Paper V of the series, we present results obtained through a series of new PRAO (pairwise) simultaneous observations at 112, 62 and 42 MHz that we compare with existing (non-simultaneous) Arecibo 327-MHz PSs. Profile polarization measurements at 327 and 62 MHz are also presented. We investigate the correlations between the fractional linear polarization, average-profile form, and the carousel circulation time. Preliminary results on the frequency dependence of the $A(2/1)$-$\hat{P}_3$ correlation were presented in Suleymanova & Rankin (2007). The observations are described in §II, and §III presents the results of the new simultaneous PRAO observations. §IV describes frequency dependent pulse-shape variations. In §V we analize the statistical distribution of circulation-time values. §VI presents the evidence for continuously increasing B-mode fractional linear polarization. A summary and conclusions are given in §VII.

II. Observations

The observations at low radio frequencies were conducted at the Pushchino Radio Astronomy Observatory (PRAO) using the BSA array at 112 MHz and the East-West arm of the DKR-1000 cross telescope at 42 and 62 MHz. Simultaneous observations were carried out at 112 and 42 MHz during the winter of 2005-2006 and at 112 and 62 MHz in 2007-2008. Signals from the linearly polarized arrays were fed to radiometers with 32×5-kHz contiguous channels at 42 MHz, 64×20-kHz channels at 62 MHz, and 96×20-kHz channels at 112 MHz. In each case, the dedispersed pulses were refered to the first (highest frequency) channel)—that is, 42.31, 62.67 and 111.87 MHz (*i.e.*, hereafter 42, 62 and 112 MHz for convenience). In that the total passband exceeded (or was a multiple of) the Faraday modulation period at each frequency, the total intensity of the dedispersed pulses provides a reasonable estimate of Stokes parameter I. For a rotation measure RM of 15.4 rad/m^2 the Faraday periods are 84, 275 and 1540 kHz at 42, 62 and 112 MHz, respectively.

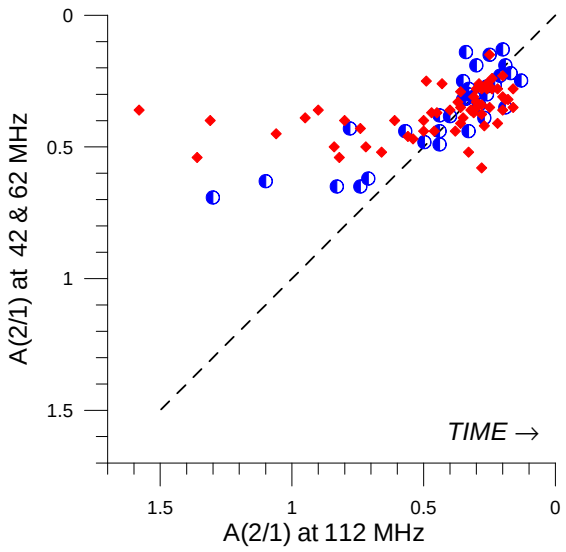

Fig. 1. Dependence of $A(2/1)$ at the lower frequencies of 42 (diamonds) and 62 MHz (open circles) *vs.* $A(2/1)$ at 112 MHz. The corresponding values track each other along the diagonal (dashed line) only within a range of about 0.1-0.5—*i.e.*, for the times closer to B-mode cessation. At all earlier times, especially during the first tens of minutes following B-mode onset, they are quite distinct. The total number of values are 59 (42/112 MHz) and 33 (62/112 MHz), which were chosen for their common good signal-to-noise ratio in both bands. Both $A(2/1)$ axes are labeled in a descending manner to indicate time increasing after B-mode onset.

Linear polarization information was available for each sample of the averaged profiles, following from the Faraday polarimetry technique developed at PRAO (Suleymanova *et al.* 1988). The fractional linear polarization was estimated from the Faraday-rotation-induced intensity modulation across the passband. Both telescopes are transit instruments and have different beam widths. The available observation time for B0943+10 is nearly 15 min using the DKR-1000 and only 4 min on the BSA array, providing PSs of 860 pulses at 42 & 62 MHz and 190 pulses at 112 MHz (see Figure 6). The total broadening of the pulse width at the half-power level in the bandwidth of single channels caused by both interstellar scattering and the receiver time constant is 7 ms (42 MHz), 5 ms (62 MHz) and

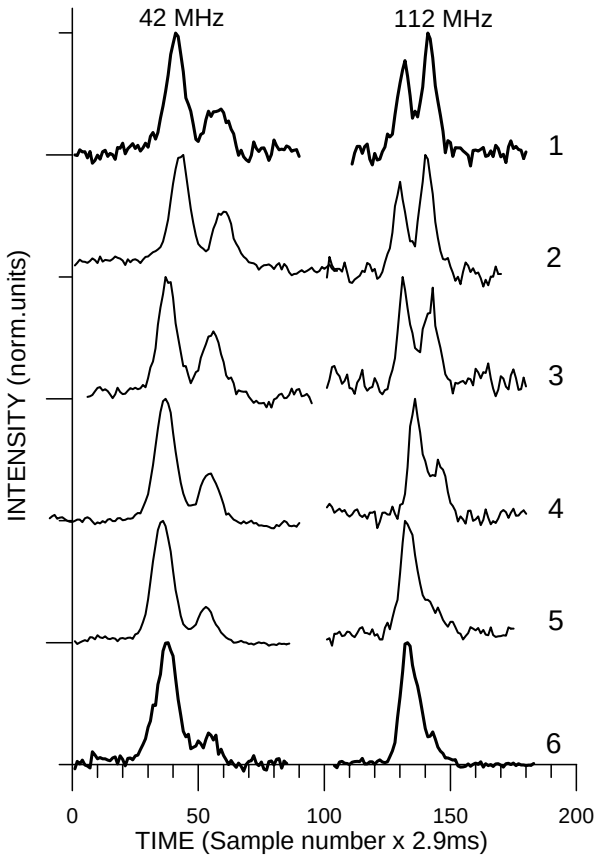

Fig. 2. The figure shows the evolution of the average pulses between B-mode onset (top) and B-mode cessation (bottom) at two simultaneous frequencies, 42 (left) and 112 MHz (right). These typical average profiles are ordered by their ascending (top to bottom) circulation times ($\hat{P}_3$). The corresponding values are given in the Table 1. Together, these show that the changes in the average-profile shape throughout the B-mode lifetime are strongly frequency dependent

3.2 ms (112 MHz). The sampling interval was 2.8762 ms at all three frequencies.

III. Simultaneous dual-band observations at 42/112 and 62/112 MHz

The observations at 42 and 112 MHz during December 2005 to January 2006, together with those at 62 and 112 MHz begining from December 2007, were conducted for a total of about 120 transits. Of these, some 59 and 33 simultaneous pulse-sequence pairs, respectively, were chosen for their good signal-to-noise ratio (hereafter S/N) in both bands. In order to investigate variations in the profile shape quantitatively, with respect to both time and frequency, the amplitude ratio $A(2/1)$ of the trailing to leading component was calculated for each average profile. The dependence $A(2/1)$ at the lower frequencies versus that at 112 MHz is then shown in Figure 1. The diagram shows that the corresponding values are correlated only within a

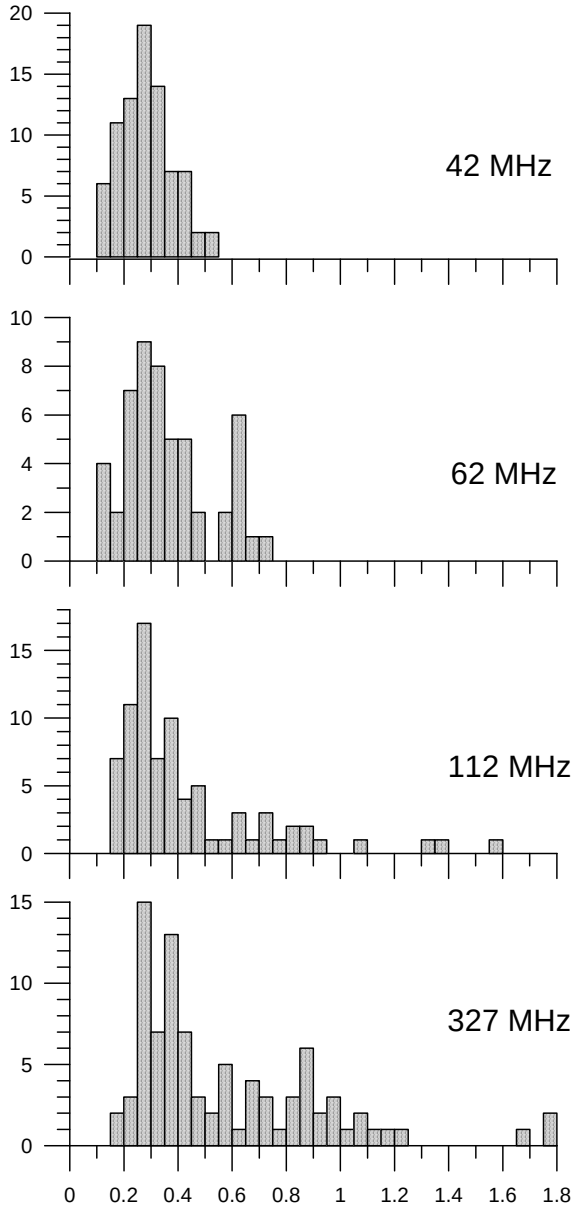

Fig. 3. B-mode histograms of the component-peak-intensity ratio $A(2/1)$ at 42, 62, and 112 MHz (PRAO, 2005-2008) together with a similarly computed 327-MHz (Arecibo, 2003) histogram. Clearly, the component-amplitude ratio $A(2/1)$ varies over a much wider range at the two higher frequencies.

range of about 0.1-0.5—which in turn corresponds to times long after B-mode onset and indeed closer to B-mode cessation. At all earlier times—corresponding to larger values of $A(2/1)$ at 112 MHz—the lower frequency $A(2/1)$ values exhibit much less variation. Note that the $A(2/1)$ values are plotted in a decreasing manner to indicate increasing time after B-mode onset.

Hereafter the temporal values were computed using circulation-time values determined from their fluctuation spectra as $\hat{P}_3$=$20/f_1$, where f_1 is the true (non-aliased) subpulse-modulation frequency. Observations at 327 MHz

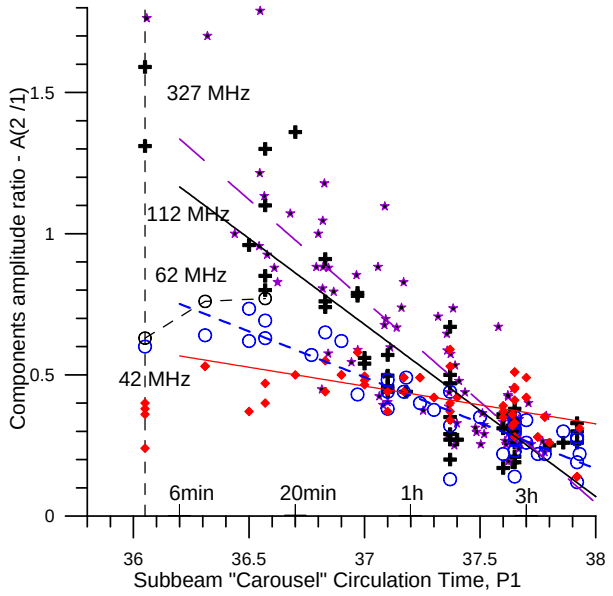

Fig. 4. Integrated-pulse-profile evolution during the 'B'urst-mode lifetime of pulsar B0943+10. The profile component-amplitude ratio $A(2/1)$ is plotted as a function of the circulation time $\hat{P}_3$ of the 20-subbeam carousel at 327 MHz (stars), 112 MHz (crosses), 62 MHz (open circles), and 42 MHz (diamonds). Each averaged profile is comprised of 256 individual pulses at 327 MHz, 190 at 112 MHz, and 860 at 42 & 62 MHz. The vertical dashed line indicates the B-mode onset time, and several other approximate B-mode timings are given along the horizontal axis.

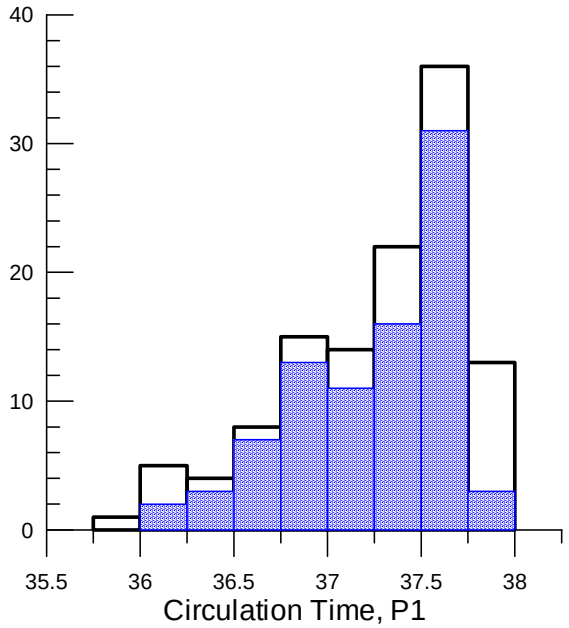

Fig. 5. Histograms of circulation time ($\hat{P}_3$) occurrence, based on the PRAO (2005-2008) observations at 112, 62 and 42 MHz as well as the Arecibo (2003) values at 327 MHz. The respective bars are shown with open and dark columns. They similarly show the increasing B-mode lifetime at larger carousel circulation times. The reversing tendency at circulation times between 37.75 and 38 P_1 is caused by the increased probability of B-mode cessations there.

Table 1. B-mode variations of A(2/1) at 42/112 MHz with $\hat{P}_3$

Number	A(2/1) 42 MHz	A(2/1) 112 MHz	$\hat{P}_3$ (P_1)	Date Date
1	0.46	1.30	36.0	21.05.05
2	0.36	1.58	36.7	10.02.05
3	0.55	0.91	36.8	16.01.06
4	0.37	0.47	37.3	07.12.06
5	0.28	0.26	37.7	04.12.06
6	0.26	0.27	37.8	01.04.06

have shown that $\hat{P}_3$ relaxes from some 36 P_1 to an asymptotic value of perhaps 38 P_1 over the course of a modal 'B'urst (Fig. 8, Paper IV). The time (in minutes) is then $1.826\text{x}10^{-32}\exp(2.077\hat{P}_3)$. This equation is independent of frequency as far as allour simultaneous dual-band measurements indicate that observationpairs exhibit small modulation frequency differencies at a level of a few standard deviations.

Figure 2 gives examples of typical averaged profiles, corresponding to successively increasing times after B-mode onset and recorded simultaneously at 42 and 112 MHz. Their values of $A(2/1)$, together with both the corresponding 20-subbeam carousel circulation times $\hat{P}_3$ and the dates of the observations are given in Table 1. Here, one need not struggle to discern the evolution of the average profile form over the entire multi-hour interval between B-mode onset (top) and B-mode cessation (bottom) at the two frequencies, 42 MHz (left) and 112 MHz (right). This full set of average profiles evidently shows that the changes in the pulse shape are more dramatic at higher frequencies.

IV. Frequency dependent $A(2/1)$-$\hat{P}_3$ correlation

Further evidence for a frequency dependence of $A(2/1)$ in relation to the circulation time $\hat{P}_3$ is given in the $A(2/1)$ histograms of Figure 3. The distributions of $A(2/1)$ values become progressively narrower at lower frequencies. In order to investigate the nature of these evident differences, we plot the component peak-amplitude ratio $A(2/1)$ versus the subbeam-circulation time for the four frequencies in Figure 4. Comparison of these $A(2/1)$ profile-shape indicators between B-mode onset and cessation reveals significant differences in the evolution at the different frequencies—*i.e.*, the changes are less dramatic at 62 and 42 MHz as compared with those at 327 and 112 MHz. The $A(2/1)$ values seem to depend linearly on $\hat{P}_3$ in the range between about 36.3 and 38 P_1.

Critical times in the B-mode evolution

It is worth noting that the $A(2/1)$ values appear to depart strongly from a linear behavior in the first minutes after

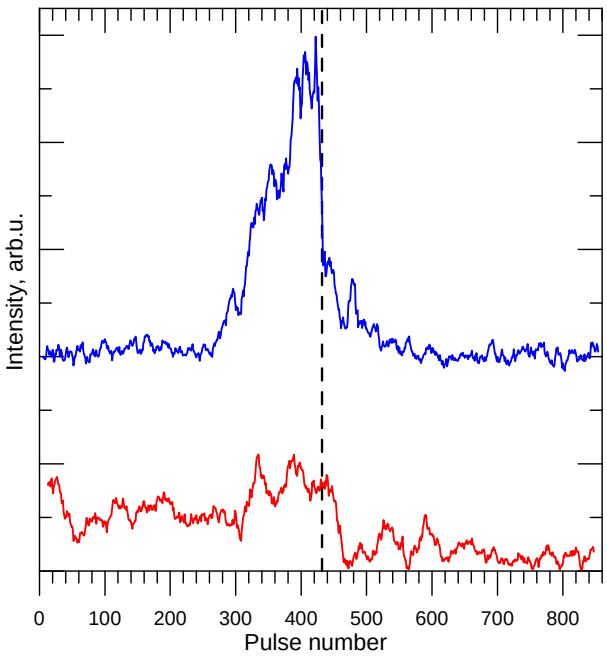

Fig. 6. Total intensity PS of B0943+10, observed through transit on 1 April 2006 using the BSA (upper) and DKR-1000 (lower plot) arrays at 112 and 42 MHz, respectively. The abrupt weakening of the intensity occurs close to the pulsar's culmination as a result of B-mode cessation. The PSs preceding cessation form profiles with component-amplitude ratios $A(2/1) \sim 0.27$ (see Fig. 2 & Table 1) and carousel-circulation times of 37.8 P_1. The PS intensities were smoothed using respective running averages of length 11 and 25 P_1 at 112 and 42 MHz so as to present the effects more clearly. The vertical dashed line marks pulse #432, the B-to-Q-mode transition point at 112 MHz—though the transition falls at pulse #460 at the lower frequency due to dispersion delay.

B-mode onset. In Fig. 4 the first five minutes relate to $\hat{P}_3$ values between 36.05 and 36.3 P_1. This effect was first noticed at 327 MHz; Paper IV, fig. 5 shows that the $A(2/1)$ values corresponding to the first 256 pulses (some 4.7 min) for the three Q-to-B-mode transition days are systematically 1.3 times larger than predicted by an exponential function that fits the great bulk of the values. This effect is also seen in Fig. 4 at both 327 and 112 MHz. In strange opposition to this, the corresponding values of $A(2/1)$ at 62 and 42 MHz are smaller than would be expected by linear fits. At the lowest frequency of 42 MHz the $A(2/1)$-$\hat{P}_3$ relation can best be described by two linear functions with different behaviors of $A(2/1)$ above and below some critical circulation time of about 36.9 P_1.

In that the effect is least evident at 62 MHz, we analyzed two observations at this frequency containing intervals of both the Q and B modes. On 8 April 2007 the Q-B-mode transition occurred at about pulse 650. The B-mode profile computed from the remaining 210 pulses (of the 860 total) was found to have an $A(2/1)$ value of 0.6 and a circulation time of 36.05 P_1. A second similar Q-B transition occurred on 2 December 2007 at pulse 100. This latter B-mode profile, comprising the last 760 pulses, has $A(2/1) = 0.73$. The fluctuation spectra for this PS exhibit triple peaks, and the corresponding circulation times are 36.05, 36.31 and 36.57 P_1. Further study of the record has revealed that these different values correspond to three sub-groups of pulses, #s 101-356, #s 357-612 and #s 603-859, which each have a distinct subpulse modulation frequency. The corresponding 256-pulse profiles in turn have $A(2/1)$ values of 0.63, 0.76, and 0.77. These values are indicated in Fig. 4 by open circles connected by a thin line. Hence, the component-peak ratio for the first 3.8 m (08.04.07) or 4.7 m (02.12.07) is less than expected from a linear extrapolation.

One can therefore conclude that the first five minutes after B-mode onset is a critical time when the difference in the pulse shape at far-separated frequencies is largest. These differencies in profile shapes at the four frequencies (as indicated by the component-peak ratio) then gradually lessens and are minimal after another critical time of about 50 min ($\hat{P}_3 = 37.1$ P_1). The third critical time of about six hours is connected to the limiting (maximum) circulation-time value.

V. On the maximum (final) circulation-time value

According to the Arecibo-2003 observations (Paper IV), the B-mode subbeam-circulation time exhibits an exponential relaxation from some 36 P_1 to an asymptotic value of perhaps 38 P_1. Just below we analyze the statistical distribution of circulation-time values based on both the PRAO-2005-2008 and Arecibo-2003 and observations. The corresponding histograms are shown in Figure 5 with open and dark columns, respectively. The total number of PSs is 117 (860 pulses in each of the scans) and 86 (256 pulses in each subaverage)—equivalent to a total of some 30.7 and 6.7 hours of B-mode observations at PRAO and Arecibo correspondingly. Remarkably, the two histograms look very similar with $\hat{P}_3$ values varying in the range between 35.92 and 37.93 (PRAO) and 36.06–37.79 (Arecibo). These histograms show that the probability of circulation-time values of $36 \div 36.75$ P_1 is the lowest, because $\hat{P}_3$ increases very rapidly during the initial 20 m after B-mode onset. The histograms exhibit a maximum circulation time of $37.50 \div 37.75$ P_1; thus the subbeam-carousel rotation may be stable for many tens of minutes or even several hours before the B again gives way to the Q mode.

The probability to encounter circulation-time values larger than about 37.7 P_1 diminishes strongly as a result of B-mode cessations. The B-to-Q-mode transition recorded at PRAO on 1 April 2006 and shown in Figure 6 supports this conclusion. The PSs preceding its B-mode cessation form profiles with component-amplitude ratios $A(2/1)$ of 0.27/0.26 (see Fig. 2 & Table 1) and exhibit a $\hat{P}_3$ value of 37.8 P_1. This value indicates that the B-to-Q transition has happened 3 hours 50 minutes after B-mode onset. On the other hand, the rightmost bar of Fig. 5 includes more that dozen circulation times that exceed this value of $\hat{P}_3$. We have examined the correspond-

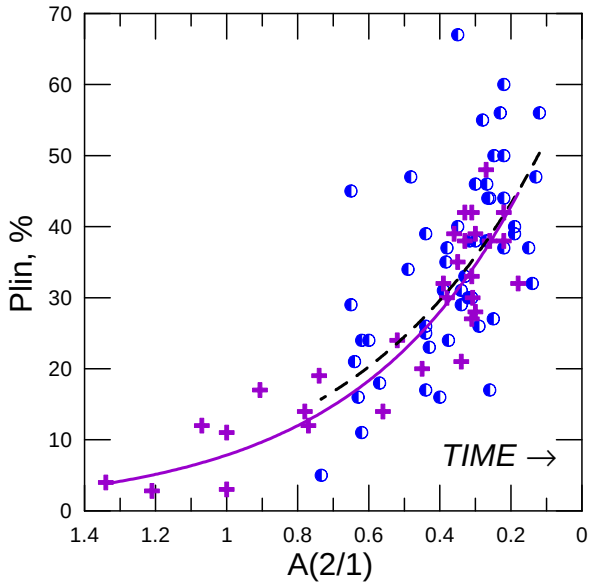

Fig. 7. Fractional linear polarization, expressed as a percentage, measured at the peak of the first component as a function of the component-amplitude ratio $A(2/1)$ of the two component peaks at 327 MHz (crosses) and 62 MHz (circles). The values are fitted to exponential functions which are marked by dashed (62 MHz) and solid (327 MHz) lines. The $A(2/1)$ scale is again given in descending order—so time since B-mode onset increases—with the values of 1.34 and 0.12 corresponding roughly to B-mode onset and cessation, respectively.

ing PSs thoroughly in an effort to identify other B-mode cessation events, but no others have been found, even at circulation times as large as 37.93 P_1. Probably a $\hat{P}_3$ value of 38.0 P_1 does represent a 'critical' period in most cases, but our experience now shows that B-mode cessation can occur over wide range of circulation times. For example, B-mode cessation was identified for the first time in the 18-m Arecibo 430-MHz PS of 19 October 1992 at a $\hat{P}_3$ of 37.35±0.02 P_1(Suleymanova *et al.* 1998, hereafter SIRR; Paper I), corresponding to B-mode life-time of 1 hour 20 minutes. Consequently, we must conclude that the duration of each individual B-mode episode can vary over a wide range from a few 10s of minutes to a few hours.

The April 1 2006 event is the second bright example of the final stage of B-mode evolution. It was detected in the course of PRAO dual-frequency observations using the BSA and DKR-1000 arrays at 112 and 42 MHz. Fig. 6 shows that the pulsar's abrupt weakening in intensity, because of B-mode cessation (marked by the vertical dashed line), occurs very close to the culmination of its transit. The individual pulses were smoothed using a running average with window widths of 11 and 25 pulses at 112 and 42 MHz, respectively. The one-sided scan from the BSA looks quite spectacular. While the vertical dashed line indicates the B-mode transition time at 112 MHz (pulse # 432), at 42 MHz the transition occurs at pulse # 460 due to dispersion delay at the lower frequency.

VI. Continuously increasing B-mode fractional linear polarization

Every analysis of B0943+10's average-profile polarization (SIRR; Papers III & IV) has shown that B-mode average profiles are more highly polarized than their Q-mode counterparts and that this circumstance results from differing proportions of power in the two polarization modes (primary/secondary; hereafter PPM and SPM); see *e.g.*, Paper IV: figs. 1 and 2. Additionally, we find a fairly wide range of fractional linear polarization in the B-mode profiles themselves, which can be anywhere in the range 20-70% at 40 & 103 MHz (Paper III). The reasons for these variations was not at all clear at the time of these earlier studies. Ongoing regular observations at PRAO have been indicating that average profiles with component-amplitude ratios less 0.3 are usually both stronger and and more highly linearly polarized. During the most recent 2007-2008 series of PRAO observations, we have accumulated statistics on these quantities at 62 MHz in order to formally assess this apparent tendency. The fractional linear polarization (given as a percentage *Plin*) was measured at the peak longitude of the stronger (leading) component I in order to provide maximum precision. These 51 values of *Plin* are plotted in Figure 7 against the component-amplitude ratio $A(2/1)$ at 62 MHz (circles). This plot exhibits very clear that *Plin* increases markedly over the lifetime of the B mode from some 5% to nearly 70%.

We thought it also interesting to investigate the linear polarization dependence at higher frequency reusing our 2003 Arecibo 327-MHz observations. Out of the six days of observations discussed in Paper IV, polarimetry was available only for MJDs 52832, 52840, and 52916-7. The first and third days contain Q-to-B-mode transitions, whereas the remaining two are 'pure B' days. Each day's several thousand pulses were divided into segments of 512 successive pulses. For most segments (a few were eliminated because of interference), the total power and total linear power profiles were available, so that the fractional linear polarization could be calculated. Here, in Fig. 7 we plot *Plin* at the peak amplitude of the leading component as a function of $A(2/1)$ (crosses). Both the 327- and 62-MHz *Plin* values are fitted by exponential functions for $A(2/1)$ taken in the range 0.18-1.34 (solid; n = 30) at 327 MHz and between 0.12-0.73 (dashed; n=51) at 62 MHz. These fitted curves reiterate that the *Plin vs* $A(2/1)$ dependence is very similar over their common range but that at 327 MHz is larger—while also somewhat clarifying the behaviour of the noisier 62-MHz values. The $A(2/1)$ axis in Fig. 7 is plotted in descending order 1.34 at B-mode onset to 0.12 at typical cessation in order to show time increasing. Our analysis confirms that *Plin* is furthermore correlated with the corresponding subbeam carousel circulations times. As shown in Figure 8, *Plin* at 327 MHz increases progressively with time following B-mode onset. A nearly linear increase of the 327-MHz component-I fractional linear polarization as a function of time is indi-

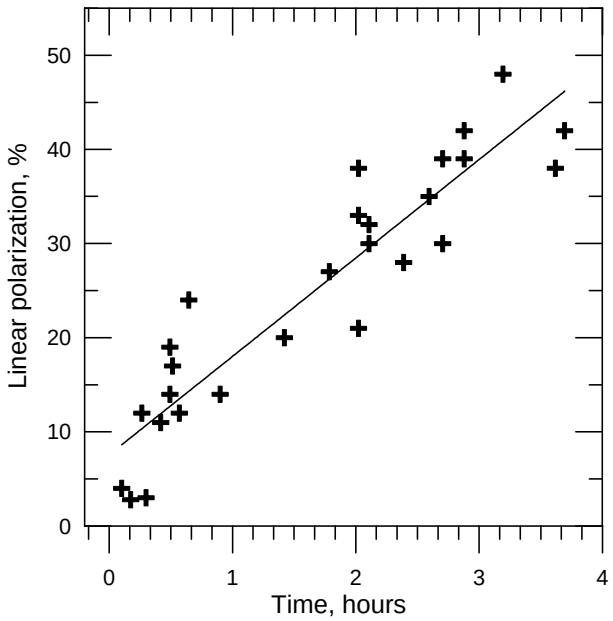

Fig. 8. Systematic dependence of the fractional linear polarization at the peak of the first (leading) component as a function of time at 327 MHz. These values were calculated as the quotient of the linear-to-total power amplitudes at the profile peak and included a correction for statistical polarization. Each average is comprised of 512 individual pulses or 9.4 min. The fractional linear polarization varies markedly within the range between about 3 and 50% over the 4+ hours between B-mode onset and cessation.

cated by the values in Fig. 8. Remarkably, the polarization changes from some 3% at B-mode onset—a value which would also be typical for the Q-mode (SIRR)—to 50% near the time of B-mode cessation.

As it was found earlier, the average B-mode profile polarization varies markedly within the range 20-70% at 40 & 103 MHz (Paper III). Now we show that day-to-day variations in the B-mode aggregate linear polarization are not sporadic in nature but correspond to different stages of B-mode evolution. Our interpretation of the phenomenon is that the continually increasing *Plin*(I) is produced by a process in which the received radiation from the pulsar is both more and more intensive and increasingly asymmetric in its contributions of PPM and SPM power—thus resulting in an increasing aggregate-profile *Plin*.

VII. Summary and Conclusions

The frequency dependence of the phenomenon suggests that propagation effects in the magnetospheric plasma may play a marked role. Petrova (2002) has shown that refraction can cause a significant redistribution of the intensity in the emission beam. As the refraction is determined mainly by the plasma-density gradient within the polar flux tube, the continuous B-mode profile-shape changes may imply a correspondingly slow redistribution of the plasma outflow. Refraction is expected to be more intense at higher frequencies, > 1 GHz, where rays are emitted nearly parallel to the local magnetic field (Lyubarski & Petrova 1998). Thus, to explain B0943+10's observed profile changes at low frequencies (327-40 MHz) by refraction, some exotic magnetic field geometry is needed such as the 'twisted up' one suggested initially in Paper III.

Geometry may also play a very strong, perhaps even dominant role. Recall from Paper I that B0943+10's observed emission is delimited by the circumstance that much or most of it is directed inside the circle of our sightline traverse and is thus unseen. Thus small changes in the emission radius, or height, produce very strong variations in the amount and character of the observed radiation. B0943+10's critical geometry thus surely accounts for its very steep radio-frequency spectrum—some $\nu^{-2.7}$ (Malofeev, 1999) as compared with the mean spectral index of $\nu^{-1.7}$ for 114 pulsars (Malofeev, 1996)—making it increasingly hard to detect above 400 MHz. Moreover the spacing between the components in the B-mode profile changes unusually rapidly between 25 and 100 MHz with a power law index of about –0.6 (SIRR). Drawing on the geometric models of Paper I, 300 MHz is the highest frequency at which our sightline crosses over the radial maximum-power point of the emission cone. Thus the radiation at frequencies higher than 300 MHz represents the outer 'skirts' of the pulsar's conal beam, and the angular dimensions of these profiles can no longer be simply related to those at lower frequencies (Rankin 1993). Both average and PS effects appear to confirm this circumstance: the pulsar's profiles at 430 (Paper I) and 1400 MHz (Weisberg *et al.* 1999) have aberrant widths, and the carousel 'beamlets' at 430 MHz are truncated on their interiors, literally cut off by the sightline traverse (Paper I)—whereas, at 111 MHz, where the emission cone and carousel angular radius is only slightly larger, 'beamlets' of a more circular form are seen.

A number of further effects may also follow from the critical sightline geometry of this 327-111-MHz band. Overall, it seems probable that the B- and Q-mode emission differs slightly in their respective radii or heights of emission, with the former being exterior (or at higher altitude) than the latter. The could account for their overall profile forms, the Q being 'single' and the B slightly 'double'. The characteristic intensity difference between the modes is also compatible with this idea: more of the 'B'right mode's radiation is directed outside the sightline circle as compared with the 'Q'uiet mode. Indeed, the difference in linear polarization is also comprehensible, given that the 'skirts' of the conal beam are characteristically depolarized by nearly equal contributions of the orthogonal polarization modes (Rankin & Ramachandran (2003); whereas the peak region is usually more unimodal and highly polarized. Thus the exterior sightline cut across the "skirts" of the low altitude Q-mode emission is depolarized, while the more interior traverse cut through the B-mode beam retains its linear polarization.

In this overall context, it is perhaps not so surprising that the observed changes over the duration of the B mode

are less dramatic at lower frequencies, as here the sightline traverses are even more internal.

Finally, we are left to understand the changes that occur over the duration of the B mode itself. It is tempting to hypothesize that this too involves small, progressive changes in the emission height or radius, such that the observed variations in average-profile form, carousel speed, intensity and polarization would result. One can even ask whether B0943+10's sightline trajectory along the very outer beam edge at 327 and 111 MHz might entail unusual effects, such as sensitively probing the actual noncircular edge of the polar cap (*e.g.*, see Arendt & Eilek 1998)—and thus accounting for the perplexing, temporally varying asymmetries in the observed emission about the fiducial longitude of the magnetic axis.

None of this, however, accounts for why the B and Q modes occur at all. Or why the 'B'urst mode exhibits such an extended, orderly and complex onset, or then suddenly and unpredictably 'breaks' so as to return the Q mode. SIRR showed that a B-to-Q modal transition seemed to have both gradual and prompt characteristics, but no comparable gradual effects have yet been identified in the now several well studied Q-to-B transitions. Some precipitating physical change would therefore seem needed to prompt the transitions between modes and perhaps the gradual changes within them. But what might this be, at B-mode onset, that causes the 'beamlets' to assume their stable and orderly 20-fold pattern—thus producing its characteristic modulation frequency—while the carousel circulation rate remains virtually unchanged across the transition? Similarly, it is difficult to understand how these suddenly orderly subpulses—but still circulating in the same orbit—could produce the dramatically altered profile form that appears at B-mode onset. And while it may be possible to understand how the profile can change with time and with the slowing carousel rate during the course of the B mode, these questions now remain very much unanswered.

Acknowledgements. This work was supported in part by US NSF grant AST 00-98685. Arecibo Observatory is operated by Cornell University under contract to the US National Science Foundation.

References

Arendt, P. N., & Eilek, J. A. 1998, astro-ph 9801257v1
Asgekar, A. A., & Deshpande, A. A. 2001, *MNRAS*, 326, 1249 (Paper II)
Deshpande, A. A., & Rankin, J. M. 1999, *Ap.J.*, 524, 1008
Deshpande, A. A., & Rankin, J. M. 2001, *MNRAS*, 322, 438 (Paper I)
Lyubarskii, Yu. E., & Petrova, S. A. 1998, *A&A*, 333, 181.
Malofeev, V. M. 1996, APS conf. Ser.,105, 271 (San Francisko press, eds. Johnston S., Walker M., Bailes M.)
Malofeev, V. M. 1999, preprint PRAO, Pushchino.
Petrova, S. A. 2002, *A&A*, 383, 1067
Rankin, J.M. 1993, *Ap.J.*, 405, 285 and A&AS, 85, 145 (ETVI)
Rankin, J. M., & Ramachandran, R. 2003, Ap.J., 590, 411
Rankin J. M., Suleymanova, S. A., & Deshpande A. A. 2003, *MNRAS*, 340, 1076 (Paper III)
Rankin J. M., & Suleymanova, S. A. 2006, *A&A*, 453, 679 (Paper IV)
Ruderman, M. A., & Sutherland, P. G. 1975, *Ap.J.*, 196, 51
Suleimanova, S. A., Volodin, Yu.V., & Shitov Yu.P. 1988, Soviet Ast.(TR: A. ZHURN.) 32, 2, 177
Suleymanova, S. A., Izvekova, V. A., Rankin, J. M., & Rathnasree, N. 1998, *J. Astr.&Astron.*, 19, 1. (SIRR)
Suleymanova S. A., & Rankin J. M. Proceedings "40 Years of Pulsars: Millisecond Pulsars, Magnetars, and More", August 12-17, 2007, McGill University, Montreal, Canada
Weisberg, J. M., Cordes, J. M., Lundgren, S. C., Dawson, B. R., Despotes, J. T., Morgan, J. J., Weitz, K. A., Zink, E. C., & Backer, D. C. 1999, *Ap.J. Suppl.*, 121, 171 (W-99)